NURR1 expression regulates retinal pigment epithelial–mesenchymal transition and age-related macular degeneration phenotypes

Pei-Li Yao[a] [ID], Vipul M. Parmar[a] [ID], Mayur Choudhary[a] [ID], and Goldis Malek[a,b,1] [ID]

Phenotypic variations in the retinal pigment epithelial (RPE) layer are often a predecessor and driver of ocular degenerative diseases, such as age-related macular degeneration (AMD), the leading cause of vision loss in the elderly. We previously identified the orphan nuclear receptor-related 1 (NURR1), from a nuclear receptor atlas of human RPE cells, as a candidate transcription factor potentially involved in AMD development and progression. In the present study we characterized the expression of NURR1 as a function of age in RPE cells harvested from human donor eyes and in donor tissue from AMD patients. Mechanistically, we found an age-dependent shift in NURR1 dimerization from NURR1-RXRα heterodimers toward NURR1-NURR1 homodimers in primary human RPE cells. Additionally, overexpression and activation of NURR1 attenuated TNF-α–induced epithelial-to-mesenchymal transition (EMT) and migration, and modulated EMT-associated gene and protein expression in human RPE cells independent of age. In vivo, oral administration of IP7e, a potent NURR1 activator, ameliorated EMT in an experimental model of wet AMD and improved retinal function in a mouse model that presents with dry AMD features, impacting AMD phenotype, structure, and function of RPE cells, inhibiting accumulation of immune cells, and diminishing lipid accumulation. These results provide insight into the mechanisms of action of NURR1 in the aging eye, and demonstrate that the relative expression levels and activity of NURR1 is critical for both physiological and pathological functions of human RPE cells through RXRα-dependent regulation, and that targeting NURR1 may have therapeutic potential for AMD by modulating EMT, inflammation, and lipid homeostasis.

epithelial–mesenchymal transition | nuclear receptors | NURR1 | retinal pigment epithelium | age-related macular degeneration

Age-related macular degeneration (AMD) is a progressive ocular disorder, which causes severe vision loss in adults over the age of 60. Its primary pathology is the accumulation of lipid- and protein-rich deposits, called drusen, between the retinal pigment epithelial (RPE) cells, nurse cells to the neurosensory retina, and the underlying Bruch's membrane (BrM) extracellular matrix (1, 2). Additionally, RPE defects are prevalent in all the clinical subtypes of AMD, including early and advanced dry and wet AMD, the latter cases of which are distinguished by the absence or presence of invading blood vessels from the choroid into the subretinal space, respectively (1, 3). Clinically, the late dry form of AMD, also termed geographic atrophy, is diagnosed in ∼80 to 90% of AMD patients. These patients experience vision loss in the central macula due to RPE cell death, often concomitant with significant loss of the overlying photoreceptors. Given that there are no effective treatments available for the early and late dry forms of the disease, there is an urgent need to develop a better understanding of the molecular mechanisms driving the pathogenesis of AMD, as well as identify potential targets as leads for developing potent therapies.

Several physiological pathways have been proposed to regulate the development and progression of AMD, including chronic inflammation, angiogenesis, oxidative stress, and lipid metabolic dysregulation (1). However, the underlying molecular mechanisms of this disease remain to be elucidated, a necessary goal in order to guide development of effective therapeutic interventions. We previously established a nuclear receptor atlas of human RPE cells and highlighted potential nuclear receptors with relevance to AMD pathogenesis (4). One candidate nuclear receptor identified was the orphan nuclear receptor-related 1 (NURR1 or NR4A2), in part due to its role in regulating a variety of biological processes—including cellular proliferation, differentiation, apoptosis, inflammation, lipid homeostasis, and metabolism (5–7)—pathways also involved in the AMD disease process. Functionally, NURR1's transcriptional activity is mediated through its binding to the NGF1-B response element (8). Additionally, it can form a

Significance

No treatments are available for dry age-related macular degeneration (AMD), the leading cause of vision loss in the elderly. Herein we characterized nuclear receptor-related 1 protein (NURR1) in human retinal pigment epithelial (RPE) cell as a function of age and disease, and found it able to modulate AMD pathogenesis via multiple mechanisms: NURR1 expression and transactivation in RPE cells decreases with age through a RXRα-dependent mechanism; NURR1 attenuates TNF-α–induced RPE epithelial-to-mesenchymal transition (EMT); and the small molecule IP7e, a potent NURR1 activator, improves retinal function, EMT phenotypes, and attenuates AMD-associated pathology in mouse models with AMD-associated pathology. These results provide insight into the molecular mechanisms of AMD and support targeting NURR1 as a potential therapeutic approach for AMD.

homodimer (NURR1-NURR1) or a heterodimer with its binding partner the retinoid X receptor (NURR1-RXR), through binding to the Nur response element (NurRE) and direct repeat 5 (DR5) binding domains, respectively. Although the natural ligand of NURR1 has yet to be characterized, several synthetic ligands have been identified capable of modulating NURR1 activity, including isoxazolo-pyridinone 7e (IP7e) (9), 1,1-bis (3′-indolyl)-1-(p-chlorophenyl) methane (C-DIM12) (10), and amodiaquine (11). To date, a large body of research has described the role of NURR1 in neurodevelopment and neuroprotection, launching the advancement of NURR1-based therapies for neurodegenerative diseases (12–14). However, whether or not NURR1 has a role in retinal diseases has not yet been considered. Indeed, only the physiological role of NURR1 in controlling differentiation and maturation of amacrine cells during retinal development has been reported on to date (15, 16). With this in mind, in the present study, we investigated the hypothesis that NURR1 is therapeutic in AMD development and progression via multiple mechanisms, including attenuating RPE epithelial-to-mesenchymal transition (EMT), decreasing inflammation in the ocular posterior pole, and modulating lipid deposition, using in vitro and in vivo approaches.

Results

NURR1 Immunolocalizes to Drusen in Dry AMD Donor Tissue and Its Expression in RPE Cells Decreases with Age. In human donor tissue from non-AMD aged donors, NURR1 immunolocalization was observed within the cone photoreceptors, RPE cells, and choroidal endothelial cells (Fig. 1 *A* and *B* and *SI Appendix,* Fig. S1). In cone photoreceptors, NURR1 colocalized with red/green-OPSIN (RG-OPSIN) (Fig. 1*A*) and in RPE cells, NURR1 partially colocalized with its heterodimer binding partner the RXRα (Fig. 1*B*). NURR1 expression was notably reduced in RPE cells in retinal cross-sections from early dry AMD patients as compared to age-matched non-AMD donors (*SI Appendix,* Table S1). No differences in NURR1 expression were evident throughout the choroid and in the choroidal endothelial cells between non-AMD and AMD donors. Noteworthy, diffuse and punctate NURR1 immunoreactivity was observed within drusen in AMD donor tissue (Fig. 1 *A* and *B* and *SI Appendix,* Fig. S1).

The most established and agreed upon risk factor for developing AMD is aging. We examined *NURR1* mRNA levels in freshly isolated RPE cells from human donor eyes aged 18 to 94 y and found *NURR1* expression decreased with advanced age (Fig. 1*C* and *SI Appendix,* Table S1). Similarly, *Nurr1* expression in RPE/choroid tissue complexes isolated from aged C57BL/6J mouse eyes was significantly lower compared to young mice (Fig. 1*D*). Furthermore, we established primary RPE (hRPE) cell culture lines from eight human donor eyes (age 15 to 93 y) (*SI Appendix,* Table S1). The fidelity of the hRPE cell lines were determined by examining the expression levels of bestrophin-1 (*BEST1*) and retinoid isomerohydrolase (*RPE65*), two RPE-specific markers (*SI Appendix,* Fig. S1D). The highest expression of *NURR1* was observed in RPE cells isolated from a 15-y-old donor (Fig. 1*E*). Human RPE cells cultured from donors aged between 43 and 60 y of age exhibited lower *NURR1* expression levels (Fig. 1*E*), as compared with cells from donors aged 76, 79, and 93 y, which demonstrated even lower *NURR1* expression than the young 15-y-old donor (Fig. 1*E*), demonstrating an overall decrease in *NURR1* expression in primary RPE cells cultured from donors over 60 y old (*P* = 0.028) (Fig. 1 *E, Inset*). With this in mind, the hRPE cell lines isolated from the 15-, 43-, 48-, and 60-y-old donors were designated as "young," and cell lines from the 76-,

79-, and 93-y-old donors were designated as "old" for further mechanistic analyses. Morphologically, nonmature (short culture period) RPE cells isolated from young donors exhibited heterogeneous morphology, while RPE cells isolated from old donors displayed homogenous spindle shape by light microscopy (Fig. 1 *F, Upper*). On the other hand, mature, postconfluent (long culture period) young and old RPE cells both demonstrated the more typical hexagonal shapes and developed tight junctions as evidenced by the ZO1 expression pattern (Fig. 1 *F, Lower*). The mature RPE cells were used throughout our study. Differential expression of NURR1 in young and old RPE cells was observed by immunocytochemistry and Western blot analysis, confirming an age-related decline in NURR1 expression (Fig. 1 *F* and *G*). Finally, treatment of RPE cells with two different potent NURR1 activating ligands, IP7e and C-DIM12, resulted in an induction of the NURR1 target gene, brain-derived neurotrophic factor (*BDNF*) (17), supporting activation of the receptor in RPE cells (Fig. 1*H*).

NURR1-NURR1 Homodimer and NURR1-RXR Heterodimer Activation Is Age-Dependent. AMD is a complex disease with multiple risk factors and pathogenic pathways contributing to its development, including but not limited to oxidative stress, lipid metabolic dysregulation, and inflammation (18–20), for which limited in vitro models are available. In order to determine if the differential expression of NURR1 with age is associated with the susceptibility of RPE cells to AMD-relevant environmental stimuli, mature primary young and old RPE cells were treated with proinflammatory agents (tumor necrosis factor [TNF]-α, lipopolysaccharide [LPS], and prostaglandin E2 [PGE2]) or lipids (α-linolenic acid [αLA], docosahexaenoic acid [DHA], and oxidized low-density lipoprotein [oxLDL]) and the homodimer (NurRE) and heterodimer (DR5) transcriptional activity of NURR1 was determined by luciferase reporter gene assays (*SI Appendix,* Figs. S1*F* and S2*A*). The concentration of each of the chemicals used in this study did not induce cell toxicity as assessed through cell viability assays (*SI Appendix,* Fig. S1*E*). Upon activation, NURR1-NURR1 homodimers on the NurRE site or NURR1-RXR heterodimers on the DR5 binding element promoted NURR1-mediated transactivation. PGE2, a stimulant of NURR1 expression, induced a 1.8-fold increase in NurRE activity relative to vehicle control in young RPE cells, but not in old RPE cells (*SI Appendix,* Figs. S1*F* and S2*A, Upper*). In contrast, DHA induced NurRE activity only in old RPE cells. Similarly, PGE2 increased DR5 activity in young RPE cells (2.4-fold), but this induction was negligible in old RPE cells (*SI Appendix,* Figs. S1*F* and S2*A, Lower*). LPS and DHA suppressed DR5 activity in young cells (0.5- and 0.4-fold, respectively), while αLA reduced DR5 activity in old cells (0.4-fold). These observations illustrate differential expression of NURR1 influences the responses of RPE cells to environmental insults through divergent binding complexes. Interestingly, TNF-α inhibited NurRE activity in both young and old RPE cells (0.4- and 0.5-fold, respectively) (*SI Appendix,* Figs. S1*F* and S2*A, Lower*). It is worth noting that although the activity driven by RXR was greater than that of NURR1 regardless of age, comparisons within nuclear receptor complexes revealed that the basal activity on the NURR1 binding site was greater in old RPE cells compared to young while the basal activity on the DR5 binding site in young RPE cells was markedly greater compared to old RPE cells (4.5-fold) (*SI Appendix,* Figs. S1*F* and S2*A, Lower*), suggesting an age-associated shift in dimerization from NURR1-RXR heterodimers toward NURR1-NURR1 homodimers.
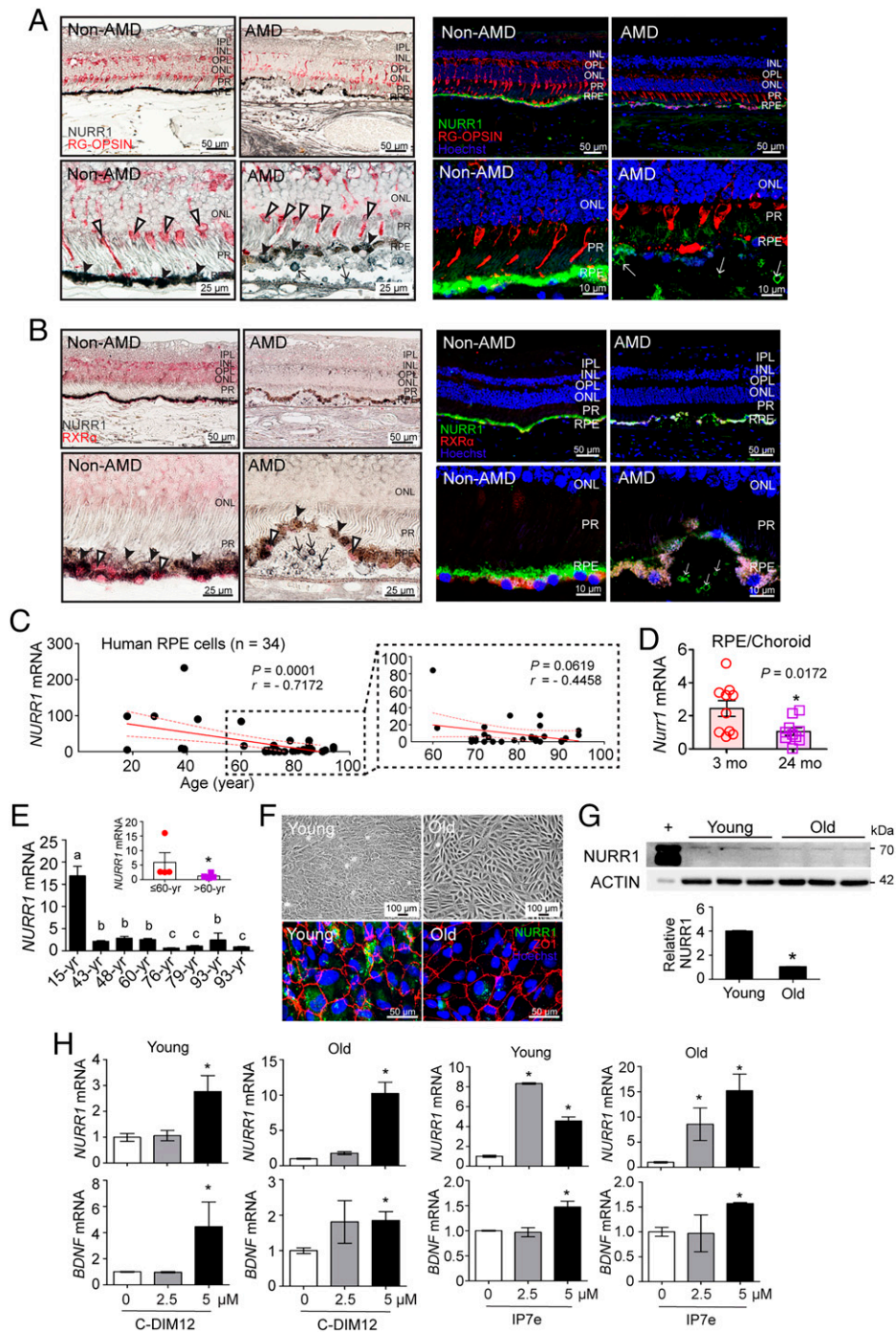
Fig. 1. NURR1 expression profile in RPE cells as a function of age and disease. Representative photomicrographs of retinal layers from aged non-AMD donors and AMD patients illustrates immunolocalization of (*A*) NURR1 and RG-OPSIN and (*B*) NURR1 and RXRα, using HRP-SG and AP-RED substrates (*Left*) shown in gray-blue and red colors, respectively, and immunofluorescence (*Right*). NURR1 is present in cone photoreceptors (white arrowheads), RPE cells (black arrowheads), and drusen (arrows). Melanin granules in RPE cells are brown. *NURR1* mRNA levels in (*C*) RPE cells freshly isolated from human donor eyes, (*D*) RPE/Choroid fractions from C57BL6/J mice and (*E*) eight hRPE cell lines (passages 4 to 8) cultured from human donor eyes (aged 15 to 93 y) as determined by qPCR. The expression of *NURR1* was normalized to that of *GAPDH* and is represented as a relative ratio to the value from ARPE-19 cells in *C* and *E*, and to 24-mo-old fractions in *D*. (*F*) Representative photomicrographs of hRPE cell morphology of nonmature RPE cell cultures from 15-y-old (young) and 93-y-old (old) donors (*Upper*) and localization of NURR1 and ZO1 in mature RPE cells (*Lower*). Hoechst staining indicates cell nuclei. (*G*) Age-dependent NURR1 expressions in hRPE cells determined by Western blot analysis and represented as a relative ratio to the old cells. ACTIN served as loading control; + is the positive control (cell lysate from HEK-293T cells transfected with human NURR1 expression vector). (*H*) Expression of *NURR1* and its target gene *BDNF* in both young and old cells in response to activating ligands, C-DIM12 or IP7e, analyzed by qPCR. Values represent mean ± SEM *Significantly different from controls using Student's *t* test, *$P \leq 0.05$. Values with different lowercase letters are significantly different from each other ($P \leq 0.05$) using ANOVA with post hoc Tukey test.

To test the hypothesis that the transactivation of NURR1-RXR heterodimers in RPE cells differs with aging, the presence of RXRα in NURR1-interacting complexes were examined by coimmunoprecipitation (co-IP) using nuclear extracts of young and old RPE cells. RXRα has previously been shown to be essential for ocular development and RPE maturation (21, 22). RXRα is also expressed in the inner nuclear layer (INL), photoreceptors (PR), and RPE cells (*SI Appendix*, Fig. S3 *A* and *B*). Although no marked difference in *RXRα* levels in RPE cells was detected across all ages, *RXRα* expression was significantly decreased with increasing age in RPE cells isolated from human donors aged over 60 y, the group with high risk of developing AMD (*SI Appendix*, Fig. S3*C*). Young RPE cells exhibited a higher basal level of NURR1 in the nucleus as compared to old RPE cells (*SI Appendix*, Fig. S2*B*). IP7e enhanced NURR1

nuclear levels in both young and old RPE cells, while C-DIM12 slightly induced NURR1 levels in old RPE cells (*SI Appendix*, Fig. S2*B*). Marked increases in RXRα expression was detected in NURR1 pull-downed complexes from young RPE cells compared to those from old cells (*SI Appendix*, Fig. S2). IP7e or C-DIM12 did not induce further changes in cellular RXRα levels. These observations reveal that NURR1 activation in young RPE cells favors the formation of NURR1-RXRα heterodimers through mechanisms yet unknown.

To further delineate the differential dimerization of NURR1 in RPE cells with age, EMSA was performed using nuclear extracts from young and old RPE cells treated with or without IP7e. Two DNA–protein complexes were detected on the DR5 binding element in both young and old control RPE cells (*SI Appendix*, Fig. S2*C*, *Left*), and the binding activity was weaker in

old control cells as compared to young control cells. The binding activity on the DR5 binding elements in the bottom complex were similar in nuclear extracts from young RPE cells treated with IP7e as compared to controls. Meanwhile, three DNA–protein complexes were formed on the NurRE binding site with nuclear extracts from young and old RPE cells (SI Appendix, Fig. S2C, Right). No visible differences in binding activities of the top and middle complexes on the NurRE binding site were observed between young and old control cells. IP7e-treated old cells, however exhibited a slight increase in the binding activity of the bottom complex on the NurRE binding site compared to young cells. A control mutant oligonucleotide displayed inhibition of binding activity.

Characterization of hRPE Cells Overexpressing NURR1. To determine whether NURR1 has a functional role in regulating the morphological and molecular phenotypes associated with AMD progression, hRPE cells (young and old) were transiently transfected with either pcDNA3.1-eGFP as mock control (Mock) or pcDNA3.1-NURR1-eGFP, to overexpress NURR1 SI Appendix, Fig. S4). Transfected cells exhibited fluorescence and their eGFP signals were routinely monitored by fluorescent microscopy (SI Appendix, Fig. S4A). The average transfection efficiency was

~83.5% as measured by flow cytometry (SI Appendix, Fig. S4B). Mature transfected cells expressed ZO1 and developed tight junctions (Fig. 2A and SI Appendix, Figs. S4B and S5A). Expression of NURR1 and its target gene BDNF increased following NURR1 overexpression in both young and old mature RPE cells (SI Appendix, Fig. S4 C and D), and overexpression of NURR1 was confirmed by Western blot analysis (Fig. 2B and SI Appendix, Figs. 4E and S5B). Noteworthy, N-CADHERIN expression was significantly reduced in both young and old RPE cells overexpressing NURR1 as compared to Mock cells (Fig. 2B and SI Appendix, Fig. S5B). In contrast, E-CADHERIN expression was increased in RPE cells overexpressing NURR1, although it did not reach significance in young cells (Fig. 2B and SI Appendix, Fig. S5B). These observations precipitated the hypothesis that modulating NURR1 expression may regulate EMT in RPE cells.

Mechanistically, an age-related difference in heterodimer versus homodimer transcriptional receptor activity was observed in NURR1 mock versus overexpressing RPE cells. The basal transcriptional activity of NURR1 on NurRE (homodimer) binding site was slightly greater in old Mock cells than young Mock cells (1.7-fold) as assessed using a luciferase reporter assay; while NURR1 activity on the DR5 (heterodimer) binding element was significantly greater in young Mock cells as compared to old Mock cells (4.9-fold) (Fig. 2C).
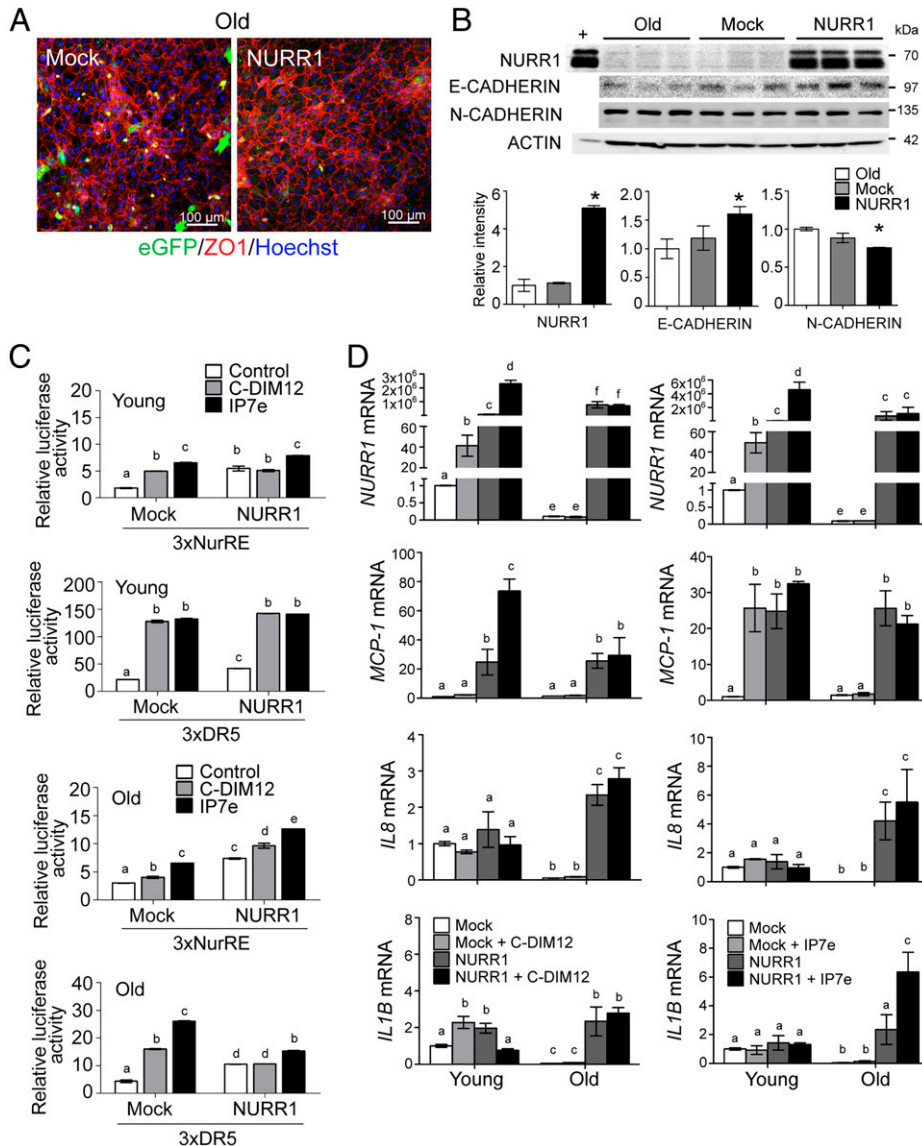

Fig. 2. Characterization of hRPE cells overexpressing NURR1. hRPE cells (young: 15-y-old donor; old: 93-y-old donor) were transiently transfected with either pcDNA3.1 empty vector (Mock) or pcDNA3.1 overexpressing plasmid carrying human NURR1 cDNA followed by the cDNA encoding eGFP protein (NURR1). (A) Representative photomicrographs of mature old cells showing positive eGFP signals in both Mock and NURR1 cells. Hoechst staining reflects cell nuclei. ZO1 staining reveals tight junction formation. (Scale bar, 100 μm.) (B) Overexpression of NURR1 in hRPE cells from old donors and its impact on the expression of E-CADHERIN and N-CADHERIN were determined by Western blot analysis; + is the positive control (cell lysate from HEK-293T cells transfected with human NURR1 expression vector). (C) Mock and NURR1 cells from young and old donors were transfected with pGL3P-luciferase plasmids carrying either 3xNurRE or 3xDR5. Cells were then treated with synthetic ligands, C-DIM12 (5 μM) or IP7e (5 μM) for 24 h. Transcriptional activities driven by NURR1-NURR1 homodimer via the 3xNurRE site or NURR1-RXR heterodimer via the 3xDR5 site were determined by luciferase reporter assays and normalized to cells transfected with a pGL3P empty vector. (D) mRNA levels of NURR1, MCP-1, IL-8, and IL-1β in Mock and NURR1 cells treated with C-DIM12 or IP7e were determined by qPCR and represented as a relative ratio to control young cells. MCP-1, monocyte chemoattractant protein 1. Values represent mean ± SEM. *Significantly different from nontransfected control group using Student's t test, *P ≤ 0.05. Values with different letters are significantly different from each other at P ≤ 0.05 using ANOVA with post hoc Tukey test.

C-DIM12 or IP7e further enhanced NURR1 activity on both the NurRE and DR5 binding sites in young and old Mock cells (Fig. 2*C*), with a more pronounced induction of activity seen following IP7e treatment on the DR5 binding site (6.4- and 6.3-fold in young and old cells, respectively). The transcriptional activity on the NurRE binding site increased in both young and old cells overexpressing NURR1 as compared to Mock cells (3.5- and 2.6-fold, respectively) (Fig. 2*C*). Similar induction in the transacting activity was observed on the DR5 binding element in both young and old NURR1 cells (2.2- and 2.8-fold, respectively); however, the increased activity in old NURR1 cells on the DR5 binding element was unable to reach the levels seen in young Mock cells. IP7e treatment stimulated an even greater induction of transacting activity on both binding sites in RPE cells overexpressing NURR1 (Fig. 2*C*), while C-DIM12-enhanced NURR1 activity was observed only on the NurRE binding site in old cells overexpressing NURR1 and on the DR5 binding element in young cells overexpressing NURR1. Interestingly, overexpression and activation of NURR1 stimulates expression of a number of cytokines—including *MCP-1*, *IL-8*, and *IL-1β*—in primary human RPE cells in an age-dependent manner (Fig. 2*D*). Collectively, these results highlight that NURR1-driven molecular activity in RPE cells varies with age.

NURR1 Activation Attenuates TNF-α–Induced EMT in Human RPE Cells. RPE cells undergoing EMT represent a morphological change to a more fibroblast-like phenotype, also observed of AMD (23, 24). To further test the hypothesis that NURR1 plays a role in EMT progression in RPE cells and determine the extent to which this may be age-dependent, the expression of EMT markers were measured in mature young and old RPE cells treated with IP7e. Basal mRNA levels of E-CADHERIN (*CDH1*), N-CADHERIN (*CDH2*), and VIMENTIN (*VIM*) were greater in young compared to old cells (Fig. 3*A*). TNF-α treatment markedly down-regulated *CDH1* expression and up-regulated *CDH2* and *VIM* in young cells (Fig. 3*A*). IP7e itself had no significant impact on the expression of these EMT markers in young cells; however, pretreatment of IP7e resulted in a reversal of TNF-α–induced changes in expression of *CDH1*, *CDH2*, and *VIM* genes (Fig. 3*A*). Changes in protein levels of CDH1 and CDH2 by TNF-α and IP7e were further confirmed by Western blot analysis (Fig. 3*B* and *SI Appendix*, Fig. S5*D*). Finally, IP7e pretreatment also reversed the effect of TNF-α on expression of several other EMT markers, including zinc finger E-box binding homeobox 1 (*ZEB1*), *SNAIL*, *SLUG*, collagen type I α 1 (*COL1A1*) and *ZO1* in old RPE cells (Fig. 3*C*), with similar results observed in young RPE cells (*SI Appendix*, Fig. S5*F*). These data support that
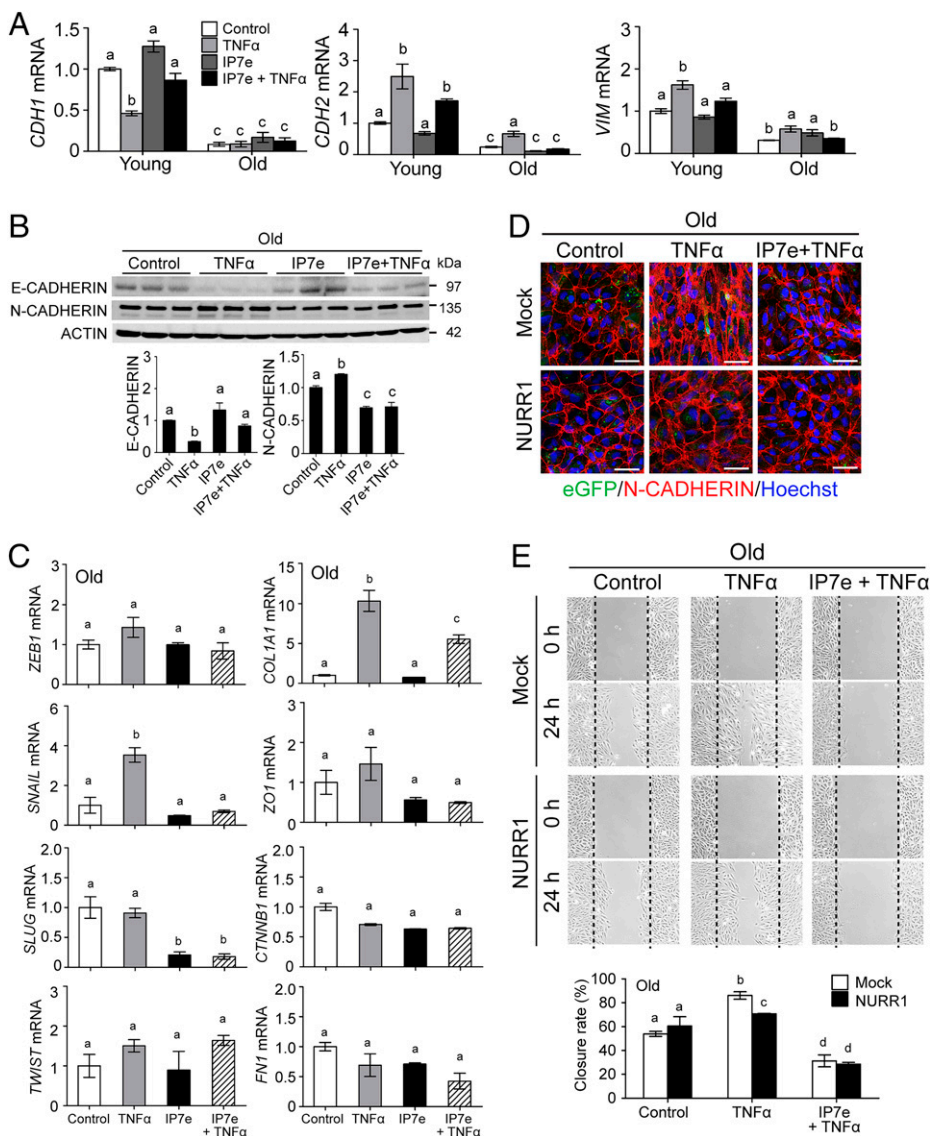

Fig. 3. Overexpression and/or activation of NURR1 attenuates TNF-α–induced EMT and hRPE cell migration. hRPE cells (young: 15-y-old donor; old: 93-y-old donor) were pretreated with IP7e for 6 h and posttreated with TNF-α for 24 h. (*A*) Expression of E-CADHERIN (*CDH1*), N-CADHERIN (*CDH2*), and VIMENTIN (*VIM*) were determined by qPCR, and represented as a relative ratio to control young cells. (*B*) Expression of E-CADHERIN and N-CADHERIN were determined by Western blot analysis. Cells were transiently transfected with either a pcDNA3.1 empty vector (Mock) or a pcDNA3.1 overexpressing plasmid carrying human *NURR1* cDNA followed by the cDNA encoding eGFP protein (NURR1). Mock and NURR1 cells were pretreated with IP7e (5 μM) for 6 h and posttreated with TNF-α (10 ng/mL) for 24 h. (*C*) Expression of EMT marker genes *ZEB1*, *SNAIL*, *SLUG*, *TWIST*, *COL1A1*, *ZO1*, *CTNNB1*, and *FN1*, in old cells were determined by qPCR and represented as a relative ratio to control cells. ZEB1, zinc finger E-box binding homeobox 1; COL1A1, collagen type I α 1; CTNNB1, β-catenin; FN1, fibronectin 1. (*D*) Representative immunofluorescence photomicrographs showing TNF-α–induced EMT as evidenced by changes in N-CADHERIN expression (red) and cell shape in old cells. The activation of NURR1 by IP7e and/or overexpression of NURR1 triggers a reversal of the EMT morphology. Hoechst staining reflects cell nuclei. (Scale bar, 50 μm.) (*E*) The effect of NURR1 overexpression or activation on cell migration as determined by a wound-healing assay. TNF-α enhanced the gap closure in mock-transfected cells, but not in cells overexpressing NURR1. Values represent mean ± SEM. Values with different lowercase letters are significantly different from each other at $P \leq 0.05$ using ANOVA with post hoc Tukey test.

the inhibitory effect of NURR1 on TNF-α–induced EMT is independent of age.

Examining the phenotype of mature RPE cells, TNF-α induced a stretched morphology in both young and old cells, and these morphological changes were diminished in cells over-expressing NURR1 and/or pretreated with IP7e (Fig. 3D and *SI Appendix*, Figs. S5C and S6A). Furthermore, a wound-healing assay demonstrated decreased cell migration in young and old RPE cells overexpressing NURR1 compared to mock controls in response to TNF-α–induced EMT (Fig. 3E and *SI Appendix*, Fig. S5E). Similar results were observed using C-DIM12 to activate NURR1 in young and old RPE cells (*SI Appendix*, Fig. S6B), as well as four additional hRPE cell lines treated with IP7e (*SI Appendix*, Fig. S7).

NURR1 Activation Improves Visual Function and Pathology in a Mouse Model with AMD Features. A recent study demonstrated the liver x receptor (LXR) is critical in NURR1-dependent dopaminergic neuron development (25). Similarly, in the present study we found knocking-down LXRα in hRPE cells suppressed NURR1 expression (Fig. 4A). Previously we demonstrated that aged Lxrα-null ($Lxra^{-/-}$) mice develop ocular pathology characteristic of the AMD phenotype (26). Thus, whether or not NURR1 is critical in visual function and may have an impact on severity of AMD pathology was investigated in adult $Lxra^{-/-}$ mice therapeutically treated with IP7e via oral gavage for 14 d. IP7e is brain penetrant and orally bioavailable (27, 28). Nurr1 expression in the RPE/choroid fractions was markedly lower, not absent, in $Lxra^{-/-}$ mice as compared to $Lxra^{+/+}$ mice (Fig. 4B). Mice treated with IP7e exhibited no changes in body weight over time and the weights of vital organs at the end of dosing period, as compared to mice treated with vehicle control, indicated no drug-associated gross adverse effects (*SI Appendix*, Table S4). Additionally, no liver damage was observed in mice exposed to IP7e, as determined by examining liver morphology, serum alanine aminotransferase (ALT) concentrations, histopathological changes in cross-sections stained with H&E, and lipid deposition in cross-sections stained with Oil red O (Fig. 4C and *SI Appendix*, Fig. S8A). IP7e treatment had no influence on serum cholesterol content (Fig. 4D). Increased expression of Bdnf and Cdh1, and decreased Slug level in RPE/choroid fractions from IP7e-treated mice indicated the activation of NURR1 in posterior pole segments of eyes following IP7e administration and the reversed EMT-signaling (Fig. 4E). Increased localization of E-CADHERIN was also detected in multiple regions of retina in IP7e-treated mice as compared to controls, including the ganglion cell layer, inner plexiform layer (IPL), outer plexiform layer (OPL), photoreceptor, and RPE (Fig. 4F).

Although optical coherence tomography (OCT) imaging did not expose gross morphological changes in the posterior pole in our mouse cohorts, fundus imaging revealed disorganized pigmentation in control adult $Lxra^{-/-}$ mice (*SI Appendix*, Fig. S8B). ERG recordings revealed that the average c-wave amplitude slightly declined in control mice at the end of dosing period, while IP7e treatment significantly enhanced the average c-wave amplitude by 43% (Fig. 4G), indicating an improvement in the RPE-dependent function. Though no significant changes were seen in the average a- and b-wave amplitudes of control mice, pre- and posttreatment in both scotopic and photopic conditions (Fig. 4 H and I), a significant improvement in scotopic b-wave, photopic a-wave, and photopic b-wave amplitudes were observed at higher flash intensities in the IP7e-treated group (Fig. 4 H and I). It is noteworthy that

sex differences in retinal function were observed, with female control $Lxra^{-/-}$ mice exhibiting significant reductions in their a- and b-wave amplitudes under both scotopic and photopic conditions by the end of dosing period, while these changes were not significant in male control mice (Fig. 4 J–L). Correspondingly, the increases in ERG amplitudes following IP7e treatment were also more pronounced in female $Lxra^{-/-}$ mice (Fig. 4 J–L).

Next, the effect of IP7e treatment on the retinal structure of $Lxra^{-/-}$ mice was investigated by evaluating their retinal morphology and histopathological features in plastic sections. Thick plastic sections stained with Toluidine blue O revealed relatively normal overall structure of posterior segments of eyes from control and IP7e-treated adult $Lxra^{-/-}$ mice (Fig. 5A and *SI Appendix*, Fig. S8C). No significant changes in the thickness of the outer nuclear layer (ONL), OPL, INL, or IPL were observed between control and IP7e groups (*SI Appendix*, Fig. S8D). Thin plastic sections examined by transmission electron microscopy (TEM) provided higher-magnification details on the ultrastructure of the outer retinal region. Adult control-treated $Lxra^{-/-}$ mice exhibited pathological abnormalities in the RPE and sub-RPE regions associated with AMD, including macro- and microvacuolization, basal laminar deposits, disrupted basal infoldings, mitochondrial changes, accumulation of lipid droplets, thickening of BrM, degenerated cellular organelle, and disorganized elastin and collagen fibers (Fig. 5 B–D, Table 1, and *SI Appendix*, Fig. S9), as reported previously (26). However, mice treated with IP7e showed more homogeneous phenotypes in the RPE with less severe pathological abnormalities (Fig. 5 B–D, Table 1, and *SI Appendix*, Fig. S9). Finally, the distribution of secondary retinal neurons was examined via immunofluorescence using cell-specific markers for Müller cells, horizontal cells, amacrine cells, and astrocytes. Expression of CALRETININ, GFAP, CRALBP, and PKCα did not appear to vary greatly in IP7e-treated mice as compared to controls (*SI Appendix*, Fig. S10). These observations support our hypothesis that IP7e treatment may be beneficial in regulating retinal function and the overall architecture of the posterior pole in AMD.

NURR1 Activation Modulates Inflammation and Lipid Homeostasis In Vivo. Immune cell infiltration and impaired lipid homeostasis in the posterior segment of eyes are hallmarks of AMD (29). IP7e administration in adult $Lxra^{-/-}$ mice markedly reduced the number of F4/80[+] or Iba1^{+} cells in RPE/choroid flat mounts and in retinal cross-sections as compared to controls as assessed by immunofluorescence (Fig. 6 A and B), indicating that activating NURR1 suppresses accumulation of immune cells in the posterior pole. Importantly, the fluorescent signal reflective of neutral lipids in the RPE and sub-RPE regions, stained by BODIPY, was diminished in IP7e-treated $Lxra^{-/-}$ mice as compared to controls (Fig. 6C). The decline in lipid deposition in the IP7e-treated cohort was associated with a significant decrease in the expression of APOE and EO6 (maker for oxidized phospholipids), as well as a slight reduction in APOB expression along the length of BrM (Fig. 6D), illustrating dysregulated lipid metabolism and accumulation of oxidized phospholipids can be diminished by NURR1 activation.

NURR1 Activation Alters the EMT Molecular Signature In Vivo in a Second Mouse Model with AMD Features. Loss of RPE differentiation has been reported in AMD and includes EMT, likely contributing to the ability of RPE cells to migrate (30). We demonstrated that IP7e treatment improved E-CADHERIN
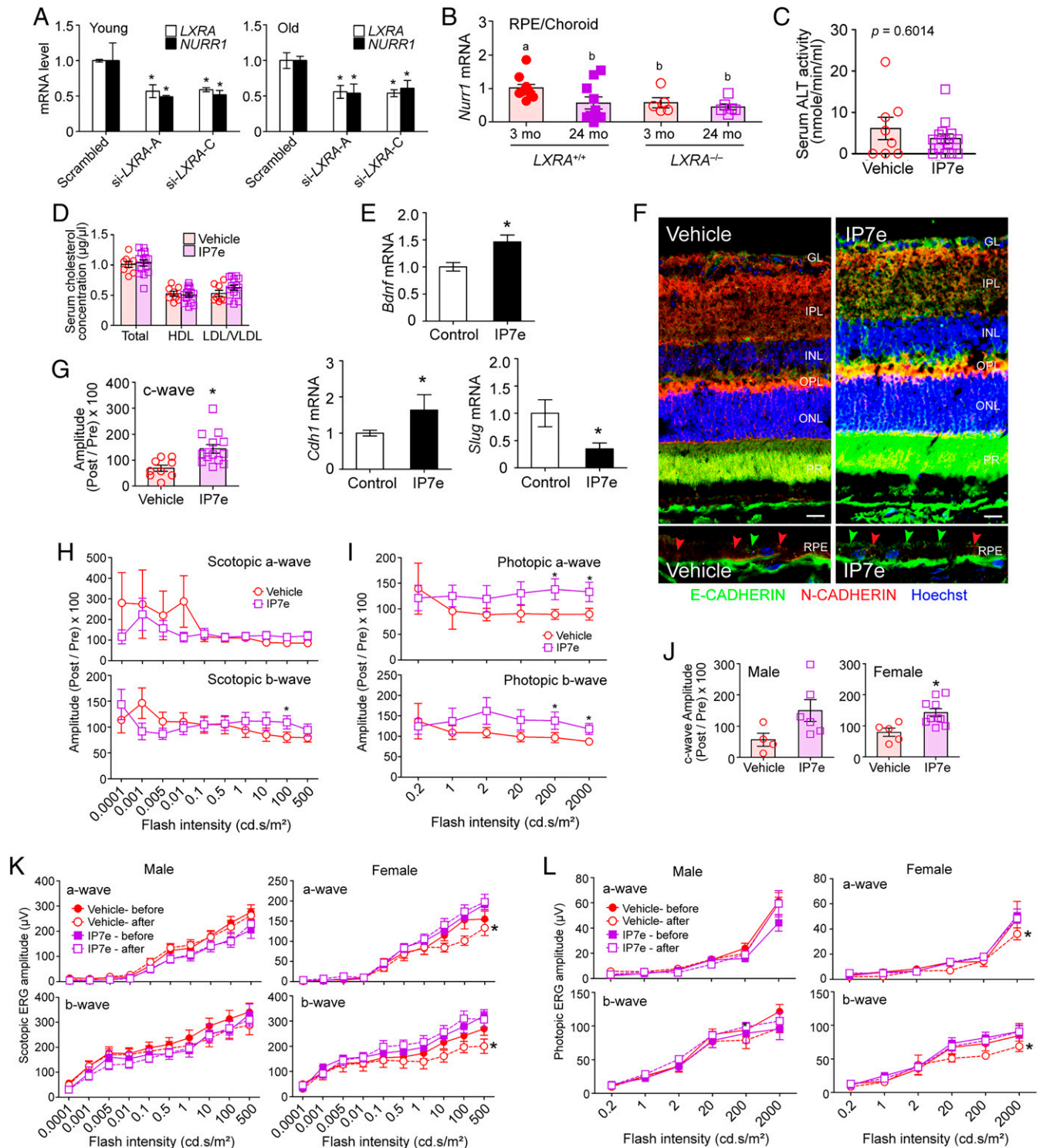
Fig. 4. The effect of NURR1 activation on retinal function and pathology in vivo. (*A*) Knocking-down of *LXRα* expression in primary cultured RPE cells (young: 15-y-old donor; old: 93-y-old donor) was achieved using siRNA. Expression of *LXRα* and *NURR1* were confirmed by qPCR. (*B*) *Nurr1* expression in RPE/Choroid fractions from *Lxra*⁺/⁺ and *Lxra*⁻/⁻ mice (3 and 24 mo old) were determined by qPCR. Adult vehicle control or IP7e (10 mg/kg) was administered twice a day by oral gavage for 14 d to *Lxra*⁻/⁻ mice (10 to 12 mo old). No significant difference in serum (*C*) ALT and (*D*) cholesterol concentration was detected between control and IP7e groups. (*E*) Expression of *Bdnf*, Cdh1, and *Slug* in RPE/choroid fractions were determined by qPCR. (*F*) Representative fluorescent photomicrographs demonstrating the immunolocalization patterns of E-CADHERIN and N-CADHERIN as examined by confocal fluorescent microscopy. (Scale bars, 50 μm.) The average ERG recordings from adult *Lxra*⁻/⁻ mice in response to IP7e treatment are shown as changes in amplitudes of (*G*) c-wave and a-, b-waves under (*H*) scotopic and (*I*) photopic conditions. ERG recordings also revealed gender differences in (*J*) c-wave amplitude, (*K*) scotopic a- and b-wave amplitude, and (*L*) photopic a- and b-wave amplitudes following IP7e exposure. Values represent mean ± SEM *Significantly different from vehicle control group using Student's *t* test, *$P \leq 0.05$. Values with different lowercase letters are significantly different from each other at $P \leq 0.05$ using ANOVA with post hoc Tukey test.

expression in the *Lxra*⁻/⁻ mice. Changes in the EMT profile of RPE cells has also been reported in a wet AMD mouse model, in which choroidal neovascularization (CNV) and ultimately fibrosis are triggered by a laser burn, which breaks through BrM (31).

Here we tested the preventive effect of NURR1 activation on the EMT molecular signature in RPE cells using the laser-induced CNV mouse model. Adult mice (7 to 9 mo old) were divided into three groups: vehicle-treated control (no CNV lesions were
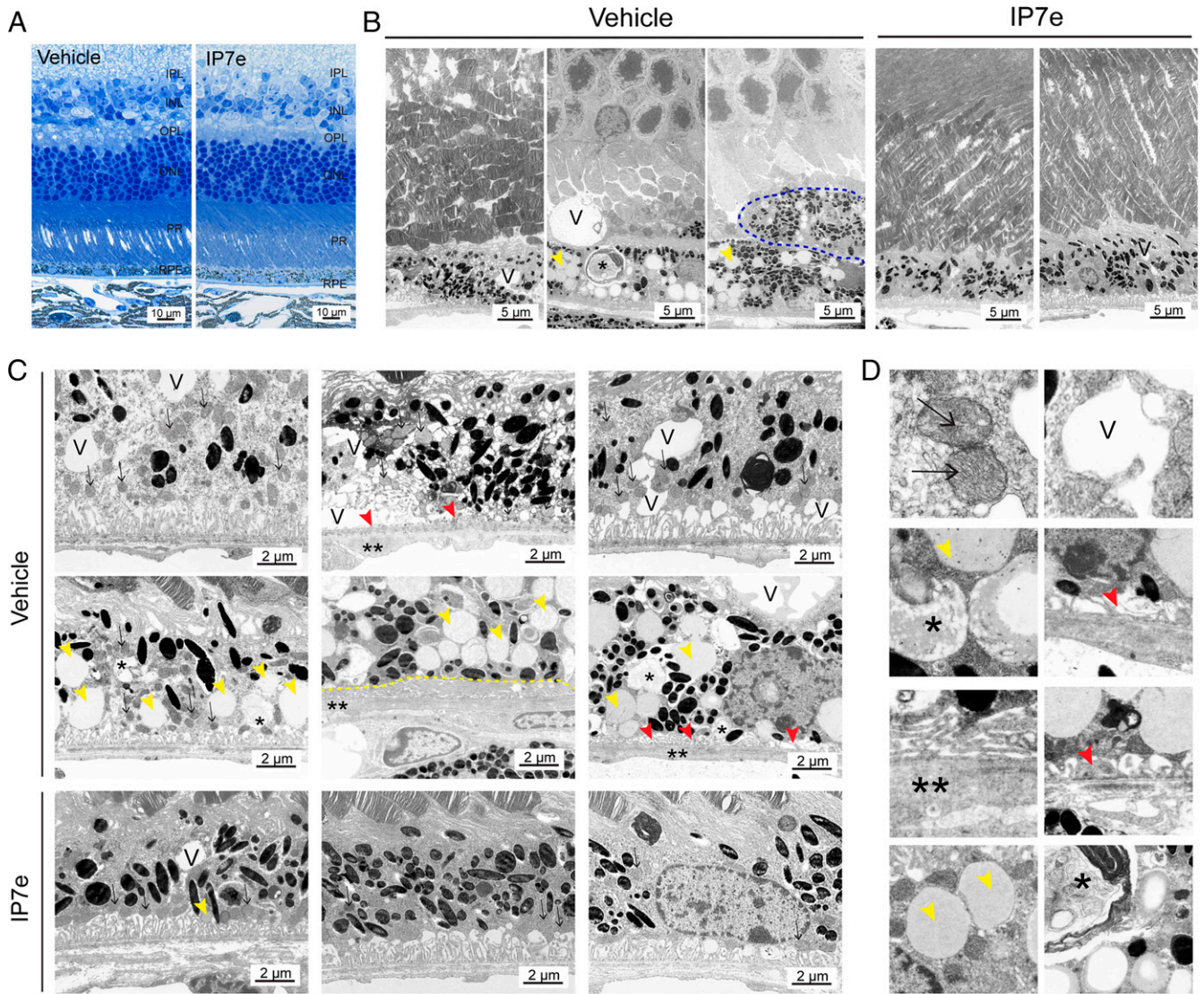
Fig. 5. Effects of IP7e treatment on retinal ultrastructure in vivo. Adult *Lxra$^{-/-}$* mice (10 to 12 mo old) received either vehicle control or IP7e (10 mg/kg) twice a day by oral gavage for 14 d. (*A*) Representative photomicrographs of the morphology of posterior pole in plastic sections (1 μm) stained with Toluidine blue O from adult *Lxra$^{-/-}$* mice treated with (*n* = 4) or without IP7e (*n* = 3). GL, ganglion cell layer. Alterations in the ultrastructure of the RPE in adult *Lxra$^{-/-}$* mice in response to IP7e treatment was examined (*B* and *C*) by TEM (magnification, 2,500× and 8,000×, respectively) and (*D*) enlarged fields of regions with abnormalities in adult control *Lxra$^{-/-}$* mice including vacuolization (V), regions with dense mitochondria (arrows), disorganized basal infoldings (red arrowheads), accumulation of lipid droplets (yellow arrowheads), extended RPE cytoplasm (blue dashed line), continuous basal laminar deposits (yellow dashed line), thickened and disorganized elastin, and collagen fibers (double asterisks) and scattered aggregates of lipofuscin-like materials or degenerated debris (asterisks) (magnification, 15,000×, respectively) shown at a magnification of 30,000×.

induced) (Fig. 7 *A, Top*); vehicle-treated plus CNV (Fig. 7 *A, Middle*); and IP7e treated plus CNV (Fig. 7 *A, Bottom*). Mice were pretreated with either vehicle or IP7e, and lasered to create 12 to 13 neovascular lesions per eye. In vivo imaging did not reveal gross differences in the lesions or retinal layers between the vehicle-treated and IP7e-treated CNV groups. Following laser-induced CNV, the expression of both epithelial markers (*E-CADHERIN* and *ZO-1*) and mesenchymal markers (*SNAIL, TWIST, α-SMA*, and *vimentin*) increased in the vehicle-treated group compared to no CNV control (Fig. 7*B*). Importantly, CNV-induced expression of these genes was diminished in the RPE of the IP7e-treated CNV group and their expression levels were similar to the no CNV control cohort, with the exception of *TWIST* and *α-SMA* levels, which remained unchanged. Additionally, an increase in *fibronectin* expression was seen in the IP7e-treated CNV cohort. These observations lend additional support to the premise that NURR1 activation may rescue the EMT-associated AMD phenotype.

Discussion

AMD is a progressive disease in the macula, presenting with complex and heterogeneous features, arising due to the interplay of genetics, environmental factors, and overall age-related health conditions in the human population. The progression of AMD and efficacy of treating wet AMD vary among affected individuals. Importantly, there are no treatment options available for the over 85% of AMD patients with the dry clinical subtype. Increasing evidence is emerging supporting functional participation of nuclear receptors in modulating ocular diseases through multiple mechanisms (32, 33). Results from the present study has elucidated pathways, by which NURR1 attenuates AMD progression, including an age-dependent switch in the composition of the transcription complex, and modulation of EMT, inflammation, and lipid metabolism in RPE cells.

RPE cells are one of the central cell types affected and vulnerable in AMD pathogenesis. We report that dry AMD

Table 1. Incidence of histopathological abnormalities in posterior segments of adult *Lxrα*⁻/⁻ mice treated with either vehicle control or IP7e

Histological parameter	Vehicle ($n = 3$)	IP7e ($n = 4$)
Photoreceptor degeneration	1/3	0/4
Retinal dysplasia	0/3	1/4
RPE degeneration		
Macrovacuolization*	3/3	1/4
Microvacuolization†	3/3	3/4
Disorganized pigment pattern	2/3	0/4
Abnormal basal infoldings	3/3	0/4
Lipid droplet accumulation	2/3	0/4
Deposit formation in sub-RPE region	2/3	0/4
Extended RPE cytoplasm	3/3	2/4
Regional thin RPE cells‡	2/3	2/4
BrM thickening§	2/3	0/4
Disorganized collagen fibers in BrM	3/3	1/4

The incidences are represented as the number of mice with the observation over the total number of mice evaluated.
*Macrovacuoles = diameter larger than 1 μm.
†Microvacuoles = diameter smaller than or equal to 1 μm.
‡Thickness of RPE less than 10 μm was recorded as thin.
§BrM thickness was measured using ImageJ. BrM thickness in vehicle control group ranged 0.39 to 2.58 μm and IP7e group ranged 0.24 to 1.06 μm.

patients exhibit a significant reduction of NURR1 expression in the RPE cell layer, supporting a possible link between NURR1 and AMD progression. The presence of NURR1 immunoreactivity in spheroids within drusen may indicate that NURR1 fragments originate from RPE cells, given a number of drusen components derive from RPE cells (34–36); however, it is also plausible that they may come from the circulation and monocytes (37). In the future it would be important to evaluate potential correlations between NURR1 expression in the RPE across the different clinical stages of AMD, as well as the circulatory profile of NURR1 as a function of age and disease.

Aging is central to the development of AMD and is an established risk factor for the disease (38). We found NURR1 expression in RPE cells declines with increasing age, consistent with a previous study demonstrating decreased NURR1 expression in the aged gerbil hippocampus (39). Functionally, NURR1 can form a homodimer or heterodimer with RXR to recognize the NurRE or DR5 binding element, respectively (8). The higher activity on DR5 binding elements in young RPE cells is associated with increased expression of NURR1 and the formation of NURR1-RXRα complexes in young cells as analyzed by co-IP and EMSA. Whether the switch from favoring the formation of NURR1-RXRα heterodimers to NURR1-NURR1 homodimers with aging is the result of a normal aging process, a consequence of the reduction of RXR expression with advanced age, or an RPE cell-specific event remains to be determined. As an orphan nuclear receptor, NURR1-mediated signaling is purported to be ligand-independent, and activation of RXR by its natural ligand, such as 9-*cis*-retinoic acid, can induce the transcriptional activity in NURR1-RXR heterodimers (8, 40, 41). Our data reveal that activation of NURR1 by small molecules, as well as AMD-relevant stressors—including TNF-α, LPS, PGE2, and αLA—triggers NURR1-specific responses, notably on DR5 binding sites, demonstrating that the interaction of NURR1-RXRα in human RPE cells is driven by age. These results, in combination with a recent study that identified the dynamic ligand binding pocket in NURR1 (42), further elevate the importance of discovering natural ligands and developing synthetic activators of NURR1 for

potential application in age-related human diseases. Interestingly, overexpression of NURR1 in old RPE cells did not fully restore the transactivation on the DR5 binding elements to the basal levels detected in young cells, suggesting that ligand binding may be critical for NURR1-RXR–mediated signaling in RPE cells.

We recently reported that aged mice carrying the null allele for *Lxra* develop functional and morphological characteristics of AMD (26). Given the fact that LXRα is also essential for NURR1-mediated signaling, we investigated the therapeutic potential of targeting NURR1 in attenuating AMD progression using adult *Lxra*⁻/⁻ mice as an AMD preclinical mouse model. We found that the small molecule IP7e activates NURR1 in the posterior segment of *Lxra*⁻/⁻ mouse eyes, and significantly improved retinal function as assessed by ERG recordings, without inducing systemic toxicity. The increase in c-wave amplitudes following IP7e treatment reflects an improvement in RPE cell function. Evaluation of the posterior pole morphology at high magnification of IP7e-treated *Lxra*⁻/⁻ mice further confirmed that NURR1 activation has therapeutic effects resolving some (though not all) of the ultrastructural features in RPE cells associated with AMD pathogenesis. Improved a- and b-waves under photopic conditions by IP7e demonstrates the functional impact of NURR1 in the neural retina (e.g., photoreceptors, bipolar cells, and Müller cells). Finally, we noted sex-based differences in the ERG amplitudes of *Lxra*⁻/⁻ mice. Striking declines in ERG amplitudes were detected in female control *Lxra*⁻/⁻ mice, and IP7e treatment in female mice abolished such reduction to a greater degree. Therefore, it is plausible that hormone regulation may play a role in regulating susceptibility to disease development and potential efficacy of therapeutics in the posterior segment of eyes when LXRα signaling is disrupted.

EMT in RPE cells delineates a phenotypic change in cell shape in response to cellular damage, ultimately contributing to wound healing, scar formation, and fibrosis, defining features seen in the late stages of AMD (23). The early phenotypic characteristics in EMT include dysregulation or redistribution of junctional proteins, reorganization of the cytoskeleton, and breakdown of polarity complex (43), controlled by a series of molecular regulators, including CADHERINs, VIMENTIN, TWIST, ZEB1, and the Zn-finger transcription factors SNAIL1 and SNAIL2 (SLUG). Previously, it has been reported that increases in NURR1 expression can diminish chemically induced fibrosis (44), a process where EMT is heavily involved (45, 46). Here we reported the inhibitory effect of NURR1 activation on TNF-α–induced EMT and migration in RPE cells in vitro, and its association with changes in expression of several EMT-related genes. The activation of NURR1 by IP7e was sufficient to rescue TNF-α–induced EMT morphologically and molecularly even in cells expressing low basal levels of NURR1. Importantly, this is consistent with our in vivo studies demonstrating that NURR1 activation in an AMD-like mouse model (*Lxra*⁻/⁻) alters expression of EMT markers in RPE/choroid fractions and improves E-CADHERIN expression in retinal cross-sections. Similarly, IP7e was able to improve the epithelial phenotype of RPE cells in a second preclinical in vivo study using the laser-induced CNV/fibrosis mouse model (47, 48). Collectively, these studies support our hypothesis that modulating NURR1 signaling may be a viable approach for the treatment of AMD by reversing the EMT process. Previous studies have identified nuclear factor erythroid 2-related factor 2 (NRF2) as a key actor against EMT and in several ocular diseases, via multiple mechanisms (23, 49). It is noteworthy that NURR1 and NRF2 can cooperatively dampen oxidative stress-induced cellular damage in midbrain dopamine-secreting neurons and macrophages (50, 51). Whether NURR1 protects against EMT in RPE
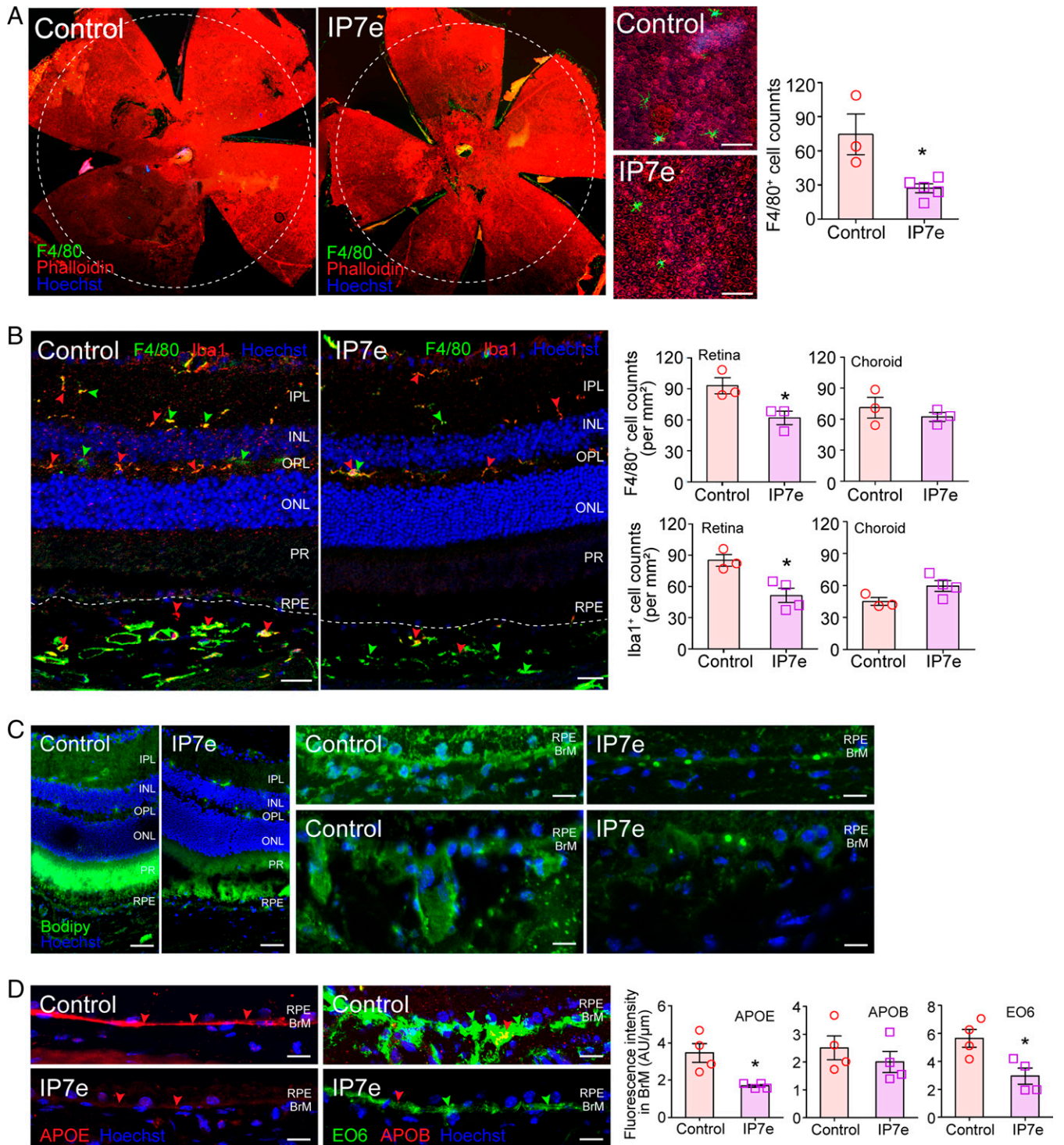
Fig. 6. The effect of NURR1 activation on distribution of inflammatory cells and lipid deposition in vivo. Vehicle control or IP7e (10 mg/kg) was administered twice a day by oral gavage for 14 d to adult *Lxra⁻/⁻* mice (10 to 12 mo old). (*A*) The presence of microglia/macrophages in RPE/choroid flat mounts were assessed by immunofluorescence using an antibody against F4/80. The area of quantified F4/80⁺ cells are indicated by white dash line. Phalloidin staining indicates actin filaments. (Scale bars, 100 μm.) (*B*) Representative photomicrographs show the localization of F4/80⁺ (green arrowheads) or Iba1⁺ cells (red arrowheads) in retinal cross-sections (10 μm) examined by immunofluorescence. IP7e treatment reduced the number of F4/80⁺ and Iba1⁺ cells in the retinal region, but not in choroid. (Scale bars, 25 μm.) (*C*) Representative photomicrographs of neutral lipid distribution in retinal cross-sections assessed by BODIPY staining. (Scale bars, 50 μm, *Left* and 25 μm, *Right*.) (*D*) Representative photomicrographs of APOE, APOB, and EO6 immunolocalization in retinal cross-sections. The fluorescent intensity was measured along BrM as an arbitrary unit (AU). Hoechst staining reflects the cell nuclei. (Scale bars, 25 μm.) Values represent mean ± SEM. *Significantly different from control group using Student's *t* test, *$P \le 0.05$.

cells by direct influence on transcriptional regulation of EMT markers or indirectly by promoting NRF2 remains to be clarified. However, NURR1 has been shown to be both pro-oncogenic or antioncogenic by modulating migration and EMT in various cancer models (52–54), highlighting that the degree to which

NURR1 modulates EMT may be cell-specific and the molecular mechanism underlying NURR1-suppressed EMT requires further examination in greater detail.

Chronic inflammation and accumulation of immune cells during the aging process are major contributors to AMD development (55,
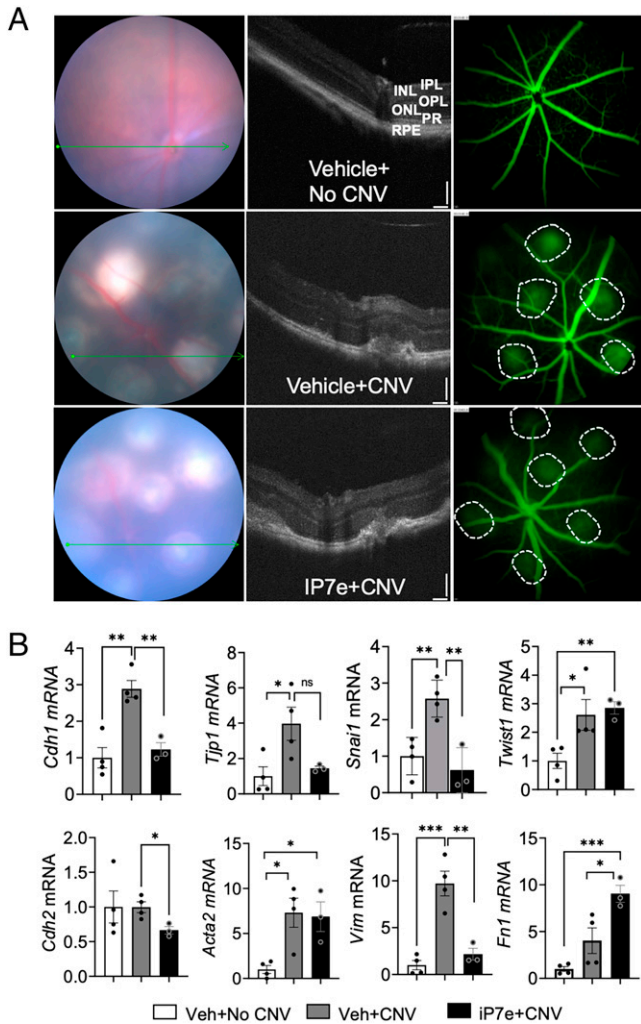
Fig. 7. Effect of NURR1 activation on EMT markers in the laser CNV mouse model. Adult C57BL6/J mice were pretreated with vehicle or NURR1 activator (IP7e) via oral gavage. Twelve to 13 thermal burns were created in the back of the eye. The no-CNV control group received vehicle by oral gavage but no laser burns. In vivo ocular evaluation of mouse eyes was conducted prior to killing. Representative images are shown. (*A*) Fundus (*Left*), OCT (*Center*), and fluorescein angiography (*Right*) images of the posterior eye in the Control (no laser, *Top*), CNV lesions in the vehicle-treated (*Middle*) and IP7e-treated (*Bottom*) groups are shown. Vascular leakage (dotted line circles) from the CNV lesions were visible by fluorescein angiography. (*B*) qPCR analysis of EMT markers epithelial markers: *Cdh1* (E-cad), *Tjp1* (ZO-1), *Snai1*, *Twist*; mesenchymal markers: *Cdh2* (N-cadherin), *Acta2* (α-smooth muscle actin), *Vim*, *Fn1*. Gene expression was normalized to that of *GAPDH* and is represented as a relative ratio. Values represent mean ± SEM (*n* = 3). *Significantly different from the control group. *$P < 0.05$; **$P < 0.01$; ns, not significant.

epithelial cells, macrophages, monocytes, mast cells, and neutrophils, among others. Importantly, they exert context-dependent effects on neuronal development, migration, plasticity, and survival (61–63). As a consequence, they have been shown to play a role in both resolution and persistence of inflammation, and have both anti- and proinflammatory properties (61–63). One may further postulate that the acute induction of proinflammatory cytokines may be necessary in order to stimulate an immune response and maintain retinal homeostasis in aged tissue (64). Alternatively, transient transfection of RPE cells may be unable to represent the dynamic interaction in the transcription complex on the chromatin, possibly leading to a different expression pattern. Case in point: a recent study found that lipofectamine-mediated transfection may trigger differential immune responses in macrophages (65). Additionally, interleukin (IL)-8 has been shown to be downstream of NURR1 in multiple models (60, 66, 67), and its expression correlates with TNF-α–dependent NF-κB signaling (60, 68). The NURR1 activator IP7e also suppresses NF-κB signaling in vivo (28). Thus, the participation of NURR1 in controlling pro- and antiinflammation is likely complicated, dependent upon the microenvironment and the physiological and pathological conditions. Finally, our findings illustrating marked inhibition of recruitment of immune cells to the retina of *Lxra*$^{-/-}$ mice following NURR1 activation in vivo on first pass may appear contradictory to the in vitro data demonstrating elevated MCP-1 levels upon NURR1 activation. However, this difference may be due to the fact that single cultured cells (e.g., RPE) versus the complex in vivo state (e.g., mouse posterior pole) are being investigated. Additionally, the MCP-1 signaling pathway has been reported to have pleiotrophic effects functioning beyond chemotaxis, potentially even regulating autophagy (69). Additional studies will be needed to determine the extent to which NURR1's regulatory effect on inflammation is driven through MCP-1 and other inflammatory regulators.

The accumulation of lipids and lipid carriers, in and extracellular to RPE cells suggests the involvement of lipid metabolic dysregulation in AMD progression (70–72). More specifically, genetic studies have consistently identified "risk genes" important in lipid and cholesterol homeostasis associated with AMD, including apolipoprotein E (APOE) (73, 74). We observed that NURR1 activation diminishes the accumulation of neutral lipids and oxidized phospholipids, and APOE expression in RPE cells of adult *Lxra*$^{-/-}$ mice. It should be noted that in a previously reported microarray analysis, APOE was identified as a NURR1 target gene in human neuroblastomas (61), suggesting NURR1-dependent regulation of APOE expression may differ between cancer and noncancer cells. Interestingly, another NURR1 activator, amodiaquine, can suppress fat mass and serum triglyceride levels, and prevent high-fat diet-induced liver steatosis (27), highlighting the need to determine the effect of different activating ligands. Furthermore, overexpression of NURR1 in macrophages has been shown to reduce oxLDL uptake and inflammation, and further attenuates atherosclerosis (75). Likely the role of NURR1 in lipid metabolism remains to be fully determined in cells with high metabolic capacity, such as hepatocytes, macrophages, and RPE cells.

In conclusion, results from the present study demonstrate that NURR1 may have a protective role in ocular diseases, in which the RPE is compromised, in part, by modulating EMT, inflammation, and lipid metabolism. Furthermore, the contribution of RXRα to NURR1 activity differs in aging and AMD, revealing a potential novel mechanism for the NURR1 signaling pathway in RPE cells.

56), and the impact of prolonged inflammation and oxidative stress on RPE degeneration has been intensively studied (57). Under normal physiological conditions, RPE cells release both immunosuppressive and inflammatory cytokines, and tightly regulate the inflammatory responses to protect against immune-mediated injury. NURR1 activation is neuroprotective and has well-known antiinflammatory effects in dopaminergic neurons, microglia, and astrocytes (11, 58, 59). Unexpectedly, we found overexpression and activation of NURR1 selectively stimulates expression of a number of cytokines—including *MCP-1*, *IL-8*, and *IL-1β*—in human RPE cells in an age-dependent manner. These cytokines were selected given NURR1's role in regulating inflammation and as several of them are known NURR1 target genes (60, 61). Though often considered proinflammatory, the nature of the cytokines we investigated are very much cell- and tissue-specific, known to target a variety of cells including endothelial cells,

Materials and Methods

Study Approval. All animal experiments were approved by the Duke University Institutional Animal Care and Use Committees. The use of human donor eyes in the present study was approved by the Duke University Institutional Review Board with an exemption.

Detailed methodology are provided in *SI Appendix, Supplementary Materials and Methods*.

Data Availability. All study data are included in the main text and/or *SI Appendix*.

Author affiliations: [a]Department of Ophthalmology, Albert Eye Research Institute, Duke University, Durham, NC 27710; and [b]Department of Pathology, Duke University, Durham, NC 27710

1. J. Ambati, B. J. Fowler, Mechanisms of age-related macular degeneration. *Neuron* **75**, 26–39 (2012).
2. W. M. Al-Zamil, S. A. Yassin, Recent developments in age-related macular degeneration: A review. *Clin. Interv. Aging* **12**, 1313–1330 (2017).
3. V. L. Bonilha, Age and disease-related structural changes in the retinal pigment epithelium. *Clin. Ophthalmol.* **2**, 413–424 (2008).
4. M. A. Dwyer, D. Kazmin, P. Hu, D. P. McDonnell, G. Malek, Research resource: Nuclear receptor atlas of human retinal pigment epithelial cells: Potential relevance to age-related macular degeneration. *Mol. Endocrinol.* **25**, 360–372 (2011).
5. J. A. Herring, W. S. Elison, J. S. Tessem, Function of Nr4a orphan nuclear receptors in proliferation, apoptosis and fuel utilization across tissues. *Cells* **8**, 1373 (2019).
6. S. Safe *et al.*, Nuclear receptor 4A (NR4A) family–Orphans no more. *J. Steroid Biochem. Mol. Biol.* **157**, 48–60 (2016).
7. R. Rodríguez-Calvo, M. Tajes, M. Vázquez-Carrera, The NR4A subfamily of nuclear receptors: Potential new therapeutic targets for the treatment of inflammatory diseases. *Expert Opin. Ther. Targets* **21**, 291–304 (2017).
8. P. Aarnisalo, C. H. Kim, J. W. Lee, T. Perlmann, Defining requirements for heterodimerization between the retinoid X receptor and the orphan nuclear receptor Nurr1. *J. Biol. Chem.* **277**, 35118–35123 (2002).
9. S. Hintermann *et al.*, Identification of a series of highly potent activators of the Nurr1 signaling pathway. *Bioorg. Med. Chem. Lett.* **17**, 193–196 (2007).
10. B. R. De Miranda *et al.*, Neuroprotective efficacy and pharmacokinetic behavior of novel anti-inflammatory para-phenyl substituted diindolylmethanes in a mouse model of Parkinson's disease. *J. Pharmacol. Exp. Ther.* **345**, 125–138 (2013).
11. C. H. Kim *et al.*, Nuclear receptor Nurr1 agonists enhance its dual functions and improve behavioral deficits in an animal model of Parkinson's disease. *Proc. Natl. Acad. Sci. U.S.A.* **112**, 8756–8761 (2015).
12. M. Jakaria *et al.*, Molecular insights into NR4A2(Nurr1): An emerging target for neuroprotective therapy against neuroinflammation and neuronal cell death. *Mol. Neurobiol.* **56**, 5799–5814 (2019).
13. M. Moon *et al.*, Nurr1 (NR4A2) regulates Alzheimer's disease-related pathogenesis and cognitive function in the 5XFAD mouse model. *Aging Cell* **18**, e12866 (2019).
14. F. Montarolo, S. Martire, S. Perga, A. Bertolotto, NURR1 impairment in multiple sclerosis. *Int. J. Mol. Sci.* **20**, 4858 (2019).
15. Y. Li *et al.*, Expression patterns of Nurr1 in rat retina development. *J. Mol. Histol.* **43**, 633–639 (2012).
16. L. Goodings *et al.*, In vivo expression of Nurr1/Nr4a2a in developing retinal amacrine subtypes in zebrafish Tg(nr4a2a:eGFP) transgenics. *J. Comp. Neurol.* **525**, 1962–1979 (2017).
17. F. Volpicelli *et al.*, Bdnf gene is a downstream target of Nurr1 transcription factor in rat midbrain neurons in vitro. *J. Neurochem.* **102**, 441–453 (2007).
18. M. Hadziahmetovic, G. Malek, Age-related macular degeneration revisited: From pathology and cellular stress to potential therapies. *Front. Cell Dev. Biol.* **8**, 612812 (2021).
19. K. L. Pennington, M. M. DeAngelis, Epidemiology of age-related macular degeneration (AMD): Associations with cardiovascular disease phenotypes and lipid factors. *Eye Vis. (Lond.)* **3**, 34 (2016).
20. Q. Xu, S. Cao, S. Rajapakse, J. A. Matsubara, Understanding AMD by analogy: Systematic review of lipid-related common pathogenic mechanisms in AMD, AD, AS and GN. *Lipids Health Dis.* **17**, 3 (2018).
21. B. Mascrez, N. B. Ghyselinck, P. Chambon, M. Mark, A transcriptionally silent RXRalpha supports early embryonic morphogenesis and heart development. *Proc. Natl. Acad. Sci. U.S.A.* **106**, 4272–4277 (2009).
22. M. Mori *et al.*, Retinal dystrophy resulting from ablation of RXR alpha in the mouse retinal pigment epithelium. *Am. J. Pathol.* **164**, 701–710 (2004).
23. J. M. T. Hyttinen *et al.*, The regulation of NFE2L2 (NRF2) signalling and epithelial-to-mesenchymal transition in age-related macular degeneration pathology. *Int. J. Mol. Sci.* **20**, 5800 (2019).
24. M. J. Radeke *et al.*, Restoration of mesenchymal retinal pigmented epithelial cells by TGFβ pathway inhibitors: Implications for age-related macular degeneration. *Genome Med.* **7**, 58 (2015).
25. P. Sacchetti *et al.*, Liver X receptors and oxysterols promote ventral midbrain neurogenesis in vivo and in human embryonic stem cells. *Cell Stem Cell* **5**, 409–419 (2009).
26. M. Choudhary *et al.*, LXRs regulate features of age-related macular degeneration and may be a potential therapeutic target. *JCI Insight* **5**, e131928 (2020).
27. L. Amoasii *et al.*, NURR1 activation in skeletal muscle controls systemic energy homeostasis. *Proc. Natl. Acad. Sci. U.S.A.* **116**, 11299–11308 (2019).
28. F. Montarolo *et al.*, Effects of isoxazolo-pyridinone 7e, a potent activator of the Nurr1 signaling pathway, on experimental autoimmune encephalomyelitis in mice. *PLoS One* **9**, e108791 (2014).
29. M. Chen, C. C. Chan, H. Xu, Cholesterol homeostasis, macrophage malfunction and age-related macular degeneration. *Ann. Transl. Med.* **6** (suppl. 1), S55 (2018).
30. M. Zhou *et al.*, Role of epithelial-mesenchymal transition in retinal pigment epithelium dysfunction. *Front. Cell Dev. Biol.* **8**, 501 (2020).
31. Y. Liu *et al.*, Suppression of choroidal neovascularization and fibrosis by a novel RNAi therapeutic agent against (pro)renin receptor. *Mol. Ther. Nucleic Acids* **17**, 113–125 (2019).
32. K. Liu, C. Zou, B. Qin, The association between nuclear receptors and ocular diseases. *Oncotarget* **8**, 27603–27615 (2017).
33. G. Malek, E. M. Lad, Emerging roles for nuclear receptors in the pathogenesis of age-related macular degeneration. *Cell. Mol. Life Sci.* **71**, 4617–4636 (2014).
34. L. V. Johnson *et al.*, Cell culture model that mimics drusen formation and triggers complement activation associated with age-related macular degeneration. *Proc. Natl. Acad. Sci. U.S.A.* **108**, 18277–18282 (2011).
35. M. Lekwuwa, M. Choudhary, E. M. Lad, G. Malek, Osteopontin accumulates in basal deposits of human eyes with age-related macular degeneration and may serve as a biomarker of aging. *Mod. Pathol.* **35**, 165–176 (2021).
36. H. Usui *et al.*, In vitro drusen model–Three-dimensional spheroid culture of retinal pigment epithelial cells. *J. Cell Sci.* **132**, jcs215798 (2018).
37. S. Fischer *et al.*, BiPSim: A flexible and generic stochastic simulator for polymerization processes. *Sci. Rep.* **11**, 14112 (2021).
38. J. R. Evans, Risk factors for age-related macular degeneration. *Prog. Retin. Eye Res.* **20**, 227–253 (2001).
39. J. H. Ahn *et al.*, Age-dependent decrease of Nurr1 protein expression in the gerbil hippocampus. *Biomed. Rep.* **8**, 517–522 (2018).
40. A. Wallen-Mackenzie *et al.*, Nurr1-RXR heterodimers mediate RXR ligand-induced signaling in neuronal cells. *Genes Dev.* **17**, 3036–3047 (2003).
41. X. C. Giner, D. Cotnoir-White, S. Mader, D. Lévesque, Selective ligand activity at Nur/retinoid X receptor complexes revealed by dimer-specific bioluminescence resonance energy transfer-based sensors. *FASEB J.* **29**, 4256–4267 (2015).
42. I. M. S. de Vera *et al.*, Defining a canonical ligand-binding pocket in the orphan nuclear receptor Nurr1. *Structure* **27**, 66–77.e5 (2019).
43. G. Moreno-Bueno *et al.*, The morphological and molecular features of the epithelial-to-mesenchymal transition. *Nat. Protoc.* **4**, 1591–1613 (2009).
44. P. Chen *et al.*, Adenovirus-mediated expression of orphan nuclear receptor NR4A2 targeting hepatic stellate cell attenuates liver fibrosis in rats. *Sci. Rep.* **6**, 33593 (2016).
45. R. Kalluri, E. G. Neilson, Epithelial-mesenchymal transition and its implications for fibrosis. *J. Clin. Invest.* **112**, 1776–1784 (2003).
46. R. C. Stone *et al.*, Epithelial-mesenchymal transition in tissue repair and fibrosis. *Cell Tissue Res.* **365**, 495–506 (2016).
47. N. Chan, S. He, C. K. Spee, K. Ishikawa, D. R. Hinton, Attenuation of choroidal neovascularization by histone deacetylase inhibitor. *PLoS One* **10**, e0120587 (2015).
48. S. M. George, F. Lu, M. Rao, L. L. Leach, J. M. Gross, The retinal pigment epithelium: Development, injury responses, and regenerative potential in mammalian and non-mammalian systems. *Prog. Retin. Eye Res.* **85**, 100969 (2021).
49. Z. Xu *et al.*, NRF2 plays a protective role in diabetic retinopathy in mice. *Diabetologia* **57**, 204–213 (2014).
50. S. M. Oh *et al.*, Combined Nurr1 and Foxa2 roles in the therapy of Parkinson's disease. *EMBO Mol. Med.* **7**, 510–525 (2015).
51. A. Kadl *et al.*, Identification of a novel macrophage phenotype that develops in response to atherogenic phospholipids via Nrf2. *Circ. Res.* **107**, 737–746 (2010).
52. S. Kang *et al.*, Anti-metastatic effect of metformin via repression of interleukin 6-induced epithelial-mesenchymal transition in human colon cancer cells. *PLoS One* **13**, e0205449 (2018).
53. S. Llopis *et al.*, Dichotomous roles for the orphan nuclear receptor NURR1 in breast cancer. *BMC Cancer* **13**, 139 (2013).
54. K. Karki *et al.*, Nuclear receptor 4A2 (NR4A2) is a druggable target for glioblastomas. *J. Neurooncol.* **146**, 25–39 (2020).
55. M. Chen, H. Xu, Parainflammation, chronic inflammation, and age-related macular degeneration. *J. Leukoc. Biol.* **98**, 713–725 (2015).
56. A. Kauppinen, J. J. Paterno, J. Blasiak, A. Salminen, K. Kaarniranta, Inflammation and its role in age-related macular degeneration. *Cell. Mol. Life Sci.* **73**, 1765–1786 (2016).
57. S. Datta, M. Cano, K. Ebrahimi, L. Wang, J. T. Handa, The impact of oxidative stress and inflammation on RPE degeneration in non-neovascular AMD. *Prog. Retin. Eye Res.* **60**, 201–218 (2017).
58. K. Saijo *et al.*, A Nurr1/CoREST pathway in microglia and astrocytes protects dopaminergic neurons from inflammation-induced death. *Cell* **137**, 47–59 (2009).
59. G. A. Smith *et al.*, A Nurr1 agonist causes neuroprotection in a Parkinson's disease lesion model primed with the toll-like receptor 3 dsRNA inflammatory stimulant poly(I:C). *PLoS One* **10**, e0121072 (2015).
60. C. M. Aherne *et al.*, Identification of NR4A2 as a transcriptional activator of IL-8 expression in human inflammatory arthritis. *Mol. Immunol.* **46**, 3345–3357 (2009).
61. M. M. Johnson, S. K. Michelhaugh, M. Bouhamdan, C. J. Schmidt, M. J. Bannon, The transcription factor NURR1 exerts concentration-dependent effects on target genes mediating distinct biological processes. *Front. Neurosci.* **5**, 135 (2011).
62. K. Giesbrecht *et al.*, IL-1β as mediator of resolution that reprograms human peripheral monocytes toward a suppressive phenotype. *Front. Immunol.* **8**, 899 (2017).
63. D. Intartaglia, G. Giamundo, I. Conte, Autophagy in the retinal pigment epithelium: A new vision and future challenges. *FEBS J.*, 10.1111/febs.16018 (2021).
64. J. M. Cicchese *et al.*, Dynamic balance of pro- and anti-inflammatory signals controls disease and limits pathology. *Immunol. Rev.* **285**, 147–167 (2018).
65. X. Guo *et al.*, Transfection reagent Lipofectamine triggers type I interferon signaling activation in macrophages. *Immunol. Cell Biol.* **97**, 92–96 (2019).
66. M. R. Davies *et al.*, Nurr1 dependent regulation of pro-inflammatory mediators in immortalised synovial fibroblasts. *J. Inflamm. (Lond.)* **2**, 15 (2005).
67. J. M. McCoy *et al.*, Orphan nuclear receptor NR4A2 induces transcription of the immunomodulatory peptide hormone prolactin. *J. Inflamm. (Lond.)* **12**, 13 (2015).
68. M. O'Kane *et al.*, Increased expression of the orphan nuclear receptor NURR1 in psoriasis and modulation following TNF-alpha inhibition. *J. Invest. Dermatol.* **128**, 300–310 (2008).
69. M. Gschwandtner, R. Derler, K. S. Midwood, More than just attractive: How CCL2 influences myeloid cell behavior beyond chemotaxis. *Front. Immunol.* **10**, 2759 (2019).
70. E. M. van Leeuwen *et al.*, A new perspective on lipid research in age-related macular degeneration. *Prog. Retin. Eye Res.* **67**, 56–86 (2018).
71. K. B. Ebrahimi, J. T. Handa, Lipids, lipoproteins, and age-related macular degeneration. *J. Lipids* **2011**, 802059 (2011).
72. R. Klein *et al.*, Lipids, lipid genes, and incident age-related macular degeneration: The three continent age-related macular degeneration consortium. *Am. J. Ophthalmol.* **158**, 513–24.e3 (2014).
73. J. Tuo, C. M. Bojanowski, C. C. Chan, Genetic factors of age-related macular degeneration. *Prog. Retin. Eye Res.* **23**, 229–249 (2004).
74. M. M. DeAngelis *et al.*, Genetics of age-related macular degeneration (AMD). *Hum. Mol. Genet.* **26** (R1), R45–R50 (2017).
75. P. I. Bonta *et al.*, Nuclear receptors Nur77, Nurr1, and NOR-1 expressed in atherosclerotic lesion macrophages reduce lipid loading and inflammatory responses. *Arterioscler. Thromb. Vasc. Biol.* **26**, 2288–2294 (2006).